⌘ *Author's Choice*

THE JOURNAL OF BIOLOGICAL CHEMISTRY VOL. 288, NO. 8, pp. 5530–5538, February 22, 2013

Immobilization of Heparan Sulfate on Electrospun Meshes to Support Embryonic Stem Cell Culture and Differentiation*[S]

Received for publication, September 28, 2012, and in revised form, November 26, 2012 Published, JBC Papers in Press, December 12, 2012, DOI 10.1074/jbc.M112.423012

Kate A. Meade[‡], Kathryn J. White[‡§], Claire E. Pickford[‡], Rebecca J. Holley[¶], Andrew Marson[‡], Donna Tillotson[‡], Toin H. van Kuppevelt[‖], Jason D. Whittle[**], Anthony J. Day[¶1], and Catherine L. R. Merry[‡2]

*From the [‡]Stem Cell Glycobiology Group, School of Materials, University of Manchester, Grosvenor Street, Manchester M1 7HS, United Kingdom, the [§]Institute of Molecular and Cellular Biology, The University of Leeds, Irene Manton Building, Leeds LS2 9JT, United Kingdom, the [¶]Wellcome Trust Centre for Cell Matrix Research, University of Manchester, Michael Smith Building, Faculty of Life Sciences, Oxford Road, Manchester M13 9PT, United Kingdom, the [‖]Department of Biochemistry, Nijmegen Centre for Molecular Life Sciences, Radboud University Nijmegen Medical Centre, 280, P.O. Box 9101, 6500 HB Nijmegen, The Netherlands, and the **Mawson Institute, University of South Australia, GPO Box 2471, Adelaide, South Australia 5001, Australia*

Background: Glycosaminoglycans influence stem cell fate but their combination with biomaterials remains to be optimized.
Results: GAG bound to scaffolds presented essential sulfation epitopes and proved biologically active.
Conclusion: Use of plasma polymerized allylamine proved effective in functionalizing a fibrous extracellular matrix mimic.
Significance: The biomaterial has broad applicability to stem cell culture and has potential future applications in regenerative medicine.

As our understanding of what guides the behavior of multi- and pluripotent stem cells deepens, so too does our ability to utilize certain cues to manipulate their behavior and maximize their therapeutic potential. Engineered, biologically functionalized materials have the capacity to influence stem cell behavior through a powerful combination of biological, mechanical, and topographical cues. Here, we present the development of a novel electrospun scaffold, functionalized with glycosaminoglycans (GAGs) ionically immobilized onto the fiber surface. Bound GAGs retained the ability to interact with GAG-binding molecules and, crucially, presented GAG sulfation motifs fundamental to mediating stem cell behavior. Bound GAG proved to be biologically active, rescuing the neural differentiation capacity of heparan sulfate-deficient mouse embryonic stem cells and functioning in concert with FGF4 to facilitate the formation of extensive neural processes across the scaffold surface. The combination of GAGs with electrospun scaffolds creates a biomaterial with potent applicability for the propagation and effective differentiation of pluripotent stem cells.

The potential benefit of pluripotent stem cells (PSCs),[3] triggering their differentiation into a specific cell type and using these for therapeutic applications fascinates scientists, clinicians, and the public. However, major hurdles remain before PSCs can fulfill this potential. Despite significant progress, protocols enabling the efficient generation of a high yield of the desired cell type are lacking and are often not fully defined, scalable, or cost effective. In particular, these requirements are all difficult to achieve given the current dependence on high concentrations of growth factors, cytokines, and matrix components (1, 2). It has long been recognized that the pericellular region, encompassing the cell surface and the immediate local extracellular matrix (ECM) has a critical role to play in directing cell behavior (3, 4); importantly, the growth of cells in two-dimensional culture, or on synthetic substrata that do not sufficiently mimic ECM, have limited utility to direct PSC fate. GAGs are linear sugars found at high concentrations in the pericellular matrix; these are displayed on core proteins (*i.e.* as part of proteoglycans) that regulate their availability and likely influence the orientation of the saccharide chains. A key function of GAGs is to modulate the activity of a wide variety of growth factors and cytokines, with factors such as the fibroblast growth factor (FGF) family, being dependent on GAGs for optimal signaling (5). Of particular importance is heparan sulfate (HS), a GAG composed of alternating hexuronic acid and glucosamine residues, which become variably sulfated during biosynthesis (6). Specific patterns of sulfated residues within the GAG chains enable the regulation of multiple binding partners, with the structural diversity of GAG sequences generating greater information carrying capability than seen in any other biological polymer, including DNA. This role of GAGs has allowed their use for PSC expansion and differentiation, with the selection of specific saccharides having the potential to enable the balanced regulation of the numerous signaling pathways directing cell behavior (7–11). However, biochemical sig-

* This work was supported by the Engineering and Physical Sciences Research Council (to K. M., A. J. D., A. M., and C. L. R. M.), the Medical Research Council (to C. L. R. M.), and The Human Frontier Science Program (to R. J. H., C. P., and C. L. R. M.).
⌘ *Author's Choice*—Final version full access.
[S] This article contains supplemental "Experimental Procedures," Table 1, Figs. 1–8, and additional references.
[1] To whom correspondence may be addressed: Wellcome Trust Centre for Cell Matrix Research, University of Manchester, Michael Smith Bldg., Faculty of Life Sciences, Oxford Rd., Manchester M13 9PT, UK. Tel.: 44-131-275-1495; E-mail: Anthony.day@manchester.ac.uk.
[2] To whom correspondence may be addressed: School of Materials, University of Manchester, Grosvenor St., Manchester M1 7HS, UK. Tel.: 44-161-306-8871; Fax: 44-161-306-8877; E-mail: catherine.merry@manchester.ac.uk.
[3] The abbreviations used are: PSC, pluripotent stem cell; GAG, glycosaminoglycans; HS, heparan sulfate; mES, mouse embryonic stem cell; ECM, extracellular matrix; ppAm, plasma polymerized allylamine; PLGA, poly(lactic-co-glycolic acid); GAG-BP, glycosaminoglycan binding protein; TSG-6, the product of tumor necrosis factor-stimulated gene-6; VSV-g, vesicular stomatitis virus G; E14, a mES cell line derived from blastocysts of strain 129/O1a mice.

nals are only part of the complex combination of factors that regulate cell behavior with topographical (12) and mechanotransductive (13) effects also playing a key role in directing differentiation. In this regard, electrospinning is a versatile and well established method of producing non-woven fiber meshes from both natural and synthetic polymers, the architecture of which can be engineered to replicate the fibrous component of the native ECM; electrospun meshes support the expansion of PSC colonies (14), aid their differentiation (12), and have been found to be amenable to functionalization with ECM protein/peptides (15) and growth factors (16). These aspects are particularly attractive considering the current difficulties in defining reproducible ECM substrata and growth factor/media combinations for PSC propagation and efficient differentiation.

Thus, presentation of GAGs within a suitable three-dimensional environment, such as electrospun meshes, offers an exciting opportunity to manipulate PSC behavior using both architectural and biological cues. However, the immobilization of complex saccharides such as GAGs onto surfaces is not a simple task as the correct three-dimensional orientation of sulfated residues is essential for their function. It may also be important for oligosaccharides to be non-covalently attached as they have been found, in some situations, to require internalization alongside signaling receptors (17). Current approaches to incorporate GAGs with biomaterials for PSC culture include the use of sulfated GAGs cross-linked into hyaluronan gels (18) or covalently immobilized onto synthetic polymer scaffolds (19). However, these methods may limit the biological activity of the bound GAGs, compromising the retention and presentation of bioactive sequences. In this study, we therefore took advantage of a means to coat GAGs onto microtiter plates (20–22), adapting this methodology, whereby cold plasma polymerization of allylamine (ppAm) onto electrospun scaffolds created a surface for the non-covalent immobilization of GAGs. This created a fibrous, ECM-mimicking mesh; a three-dimensional environment, in which selected GAGs were used to influence cell behavior. Importantly, we have used a variety of biochemical/biophysical techniques to characterize the GAGs immobilized on the surface, ensuring their display in a biologically relevant and active state. As the composition and structure of HS has proved fundamental in regulating PSC behavior (7–9, 11), it is of significance that the three-dimensional structure of the GAGs are presented and retained in this system. Therefore, by anchoring functional HS to electrospun scaffolds, it is possible to replicate and manipulate the native regulation of progenitor cells by their pericellular environment.

EXPERIMENTAL PROCEDURES

Scaffold Preparation—Electrospun microfiber poly(lactic-*co*-glycolic acid) (PLGA) scaffolds were created as described previously (23). These were ppAm-coated by cold plasma polymerization using allylamine monomers (20). For details, see supplemental "Experimental Procedures." For scanning electron microscopy (SEM) analysis, scaffolds were gold splutter-coated and analyzed on a Zeiss EVO60 VPSEM with a 5-kV accelerating voltage and a 10-cm working distance. Fiber diameter was measured using Image Tool (version 3.0).

X-ray Photoelectron Spectroscopy—X-ray photoelectron spectroscopy analysis was conducted to define the surface composition of the uncoated and ppAm-coated PLGA scaffolds as described in the supplemental "Experimental Procedures."

Disaccharide Composition Analysis—HS was immobilized by incubating 1-cm^2 sections of scaffolds in 500 μl of PBS containing 0.5, 1, 2, and 5 μg of Celsus HS (Iduron) overnight. Samples were washed in PBS before incubation with 4 M NaCl for 30 min; based on previous research, this would be expected to completely release all of the immobilized GAG (20, 21). The detached HS was desalted and the HS composition and quantification in comparison with a known quantity of HS was analyzed as described previously (24, 25). Because the efficiency of AMAC labeling varies according to specific disaccharides, the raw peaks were multiplied by predetermined correction factors (24).

Detection of Functional HS with GAG-BP—The biotinylated Link module from human TSG-6 (bA-Link_TSG6 (26) denoted here as GAG-BP), a well characterized GAG-binding domain (27), was used in a colorimetric assay to determine the amount of functional heparin/HS adsorbed onto 0.6-cm^2 uncoated and ppAm scaffolds as described previously for two-dimensional surfaces (20–22, 28). For details, see supplemental "Experimental Procedures."

Phage Display ScFv Antibody Binding—VSV-G tagged anti-heparin/HS binding antibodies NS4F5, HS4C3, and RB4EA12 were made as described previously (29). Sections of ppAm scaffolds (0.6 cm^2) were treated essentially as described for GAG-BP in supplemental "Experimental Procedures;" for binding assays with NS4F5 and HS4C3, scaffolds were incubated with 0–5 μg of heparin, whereas to assess differential binding of RB4EA12, ppAm scaffolds were incubated with 0–200 ng of HS derived from wild type E14 mES cells (derived from blastocysts of strain 129/O1a mice) or *Sulf1*$^{-/-}$/*Sulf2*$^{-/-}$ mES cells derived in-house (purified as described in Ref. 25). E14 mES cells were provided by Professor Austin Smith. For full details, see supplemental "Experimental Procedures."

Neural Differentiation—*Ext1*$^{-/-}$ mES cells (30) were donated by professor Dan Wells and maintained as described previously (7, 9). For differentiation experiments, 2.25-cm^2 sections of uncoated and ppAm scaffolds were UV-sterilized and mounted in 24-well plates using CellCrowns (Scaffdex). Scaffolds were incubated overnight at room temperature with 1 μg/cm^2 HS in PBS or PBS alone; these were washed twice with PBS before preconditioning with 1 ml of complete mES cell medium overnight at 37 °C. Cells (*Ext1*$^{-/-}$ cells and Wt1 mES cells) were seeded onto the scaffolds at 1×10^4 cells/cm^2. After 24 h, cells were washed, and medium was replaced with 1 ml of N2B27 neural differentiation medium (31). N2B27 medium was supplemented with 2 ng/ml FGF4 (BioSource) as required.

Immunocytochemistry—Cells were fixed with 4% (w/v) paraformaldehyde (Sigma) and stained for the neuronal marker βIII-tubulin as described previously (7).

[^{3}*H]HS Analysis*—Metabolically labeled [^{3}H]HS was produced from immortalized mouse embryonic fibroblasts as described previously (32, 33). To determine the rate at which bound HS detaches from the scaffolds, 1-cm^2 sections of ppAm and uncoated scaffolds were UV-sterilized and incubated over-

night with 10,000 cpm [^{3}H]HS in 1 ml of PBS. Unbound [^{3}H]HS was removed, and scaffolds were washed twice with PBS followed by incubation in 1 ml of PBS at 37 °C, 5% CO_2. PBS was changed every 2 days. At intervals, scaffolds were washed twice and analyzed for ^{3}H activity on a Wallac 1409 Liquid Scintillation counter. The percentage of bound [^{3}H]HS was calculated from the total [^{3}H]HS detected on each individual scaffold section and in all PBS washes/exchanges over the 10-day period.

Flow Cytometry—Wild type E14 mES cells and *Sulf1*$^{-/-}$*2*$^{-/-}$ mES cells were stained with ScFv antibody RB4EA12 for flow cytometry as described previously (8). Briefly, cells were harvested using cell dissociation (Invitrogen) and resuspended in PBS. Cells were incubated with RB4EA12 (1:100 dilution) followed by incubation with phycoerythrin-conjugated anti-mouse IgG1. Cells were washed twice with PBS between antibody incubations. Both antibodies were applied to the cells in PBS supplemented with 0.1% (w/v) sodium azide, 0.2% (w/v) BSA for 1 h at 4 °C. After staining, cells were fixed in 1% (v/v) formaldehyde and analyzed using a Becton Dickinson FACScalibur cell sorter (Becton Dickinson).

Statistical Analysis—The composition of bound HS applied at 1, 2, and 5 μg were tested against prebound HS using two-tailed *t* tests assuming equal variance with a 5% significance level. *p* values are provided in the appropriate figure legends.

RESULTS

Electrospun Microfiber Meshes Have Similar Dimensions to the Fibrous Components of Natural ECM—Electrospinning of PLGA created a reproducible scaffold with fiber diameter predominantly between 0.1–1.2 μm (Fig. 1*A*), dimensions that mimic those within the natural ECM (34). ppAm did not alter average fiber diameter or morphology (Fig. 1*B*) with no discernible difference between the fiber diameter distribution of coated and uncoated microfiber scaffolds.

Allylamine-coating Technology Is Transferrable to a Three-dimensional Scaffold—Scaffolds coated with ppAm were more hydrophilic (wettable) than uncoated microfiber meshes, as determined by water contact analysis (supplemental Fig. 1). X-ray photoelectron spectroscopy analysis confirmed the altered surface chemistry, with ppAm causing a marked decrease in oxygen content (from 36.81% to 5.28%) and introducing nitrogen (16.24%) (supplemental Table 1). High-resolution analysis of the core C 1 s signal of uncoated scaffolds revealed three peaks at intervals of 2 eV, corresponding to C-H, C-O, and C(=O)-O groups within the polymer chain (Fig. 2), consistent with previous research (35, 36). Plasma polymerization of allylamine introduced a broad peak at +1.5 eV relative to the C-H signal, which corresponds to C-N/C-O/C=N environments within the ppAm layer. This is consistent with previous research and indicates the presence of amines, imines and amides (35, 37) as reported for ppAm-treated plates utilized for GAG immobilization (20). From this analysis, it is clear that PLGA scaffolds can be successfully coated with ppAm.

Structurally Diverse HS Chains Can Bind to ppAm-coated Scaffolds in a Non-selective Manner—To assess whether the deposited ppAm layer could immobilize HS on the fiber surface, microfiber meshes were incubated with a range of HS concentrations in PBS overnight. Bound HS was then removed for

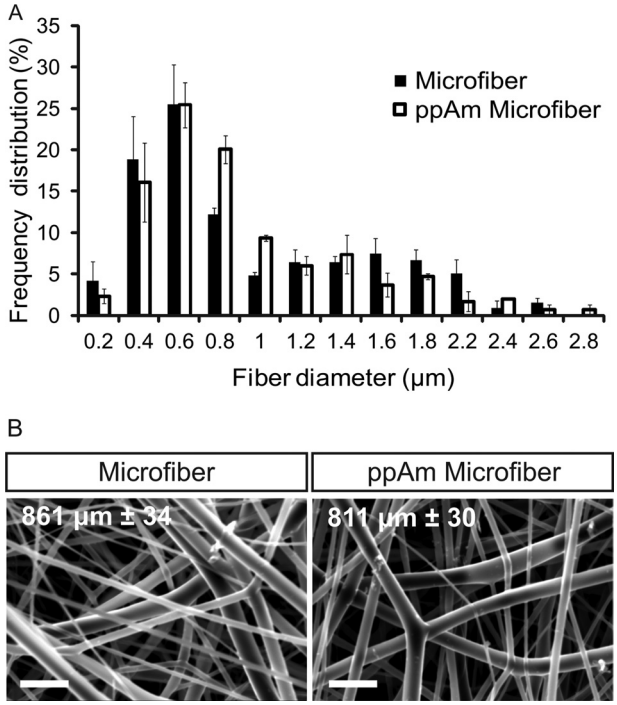

FIGURE 1. **Analysis of microfiber and ppAm microfiber scaffolds.** *A*, fiber diameter distribution of uncoated and ppAm-coated microfiber meshes. Analysis reveals no discernible difference in fiber diameter distribution between uncoated and ppAm-coated meshes. Fiber diameter for ppAm-treated scaffolds was calculated from a single mesh before and after coating. A total of at least 100 fibers were measured from three separate fields of view. Values indicate the average frequency distribution calculated from the three fields of view ($n = 3$) with *error bars* indicating S.E. Fiber diameter predominantly ranges between 0.1–1.2 μm. *B*, SEM analysis of microfiber meshes before and after ppAm coating reveal no alteration of fiber diameter or surface texture; values indicate average fiber diameter, and S.E. was calculated from a single sheet of scaffold before and after coating with ppAm. *Scale bars*, 4 μm.

analysis using a concentrated salt solution, indicating HS was immobilized via non-covalent ionic interactions and in agreement with our previous studies (20). This GAG bound the scaffolds in a dose-dependent manner with a maximum of 2.1 μg ($\pm$ 0.19) per 1 cm^2 from 5 μg of HS applied (supplemental Fig. 2*A*). The HS used here (as is the case for all HS preparations from natural sources) is composed of a diverse mixture of sequences with some chains within the population containing more overall sulfation compared with others (6). At low concentrations of applied HS (1, 2 μg/cm^2), binding is largely non-selective across this population with the overall composition of bound *versus* applied HS being similar (Fig. 3 and supplemental Fig. 2*B*). However, when the highest concentration of HS (5 μg) was applied to the scaffolds binding became selective, with a significantly greater proportion of highly sulfated residues evident within the bound material compared with the composition of HS applied. Therefore, if suitable coating concentrations are used ($<$2 μg/cm^2) a wide range of different HS sequences can be immobilized onto the ppAm-coated scaffolds in a non-biased manner.

HS Immobilized on the ppAm-coated Scaffolds Retains Specific Ligand Binding Capability—The biotinylated Link module of human TSG-6 (denoted here as GAG-BP) binds heparin, HS, chondroitin sulfate, dermatan sulfate, and hyaluronan and has been used previously to characterize GAG immobilization on

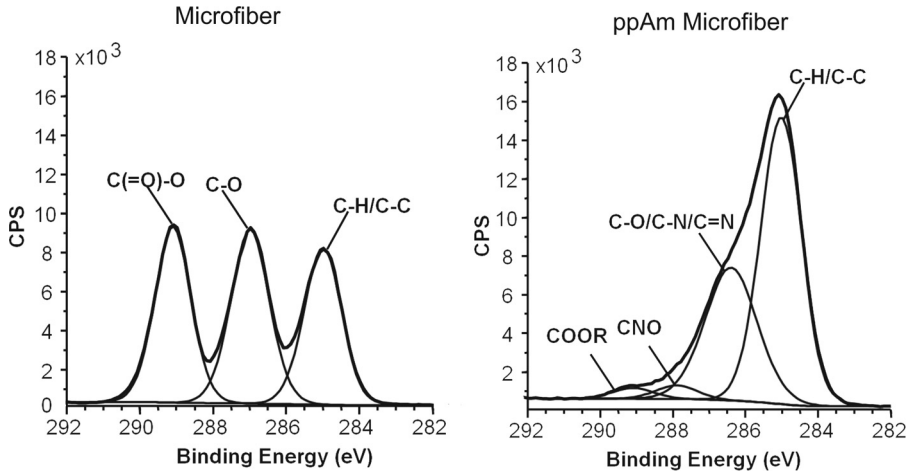

FIGURE 2. **X-ray photoelectron spectroscopy analysis of uncoated and ppAm microfiber meshes.** The core C1s signals are representative of uncoated (two separate meshes analyzed) and ppAm scaffolds (seven separate meshes analyzed). *Vertical axis* represents counts per second (*CPS*). Peaks were fitted based on previous studies (20, 22, 35–37) revealing a dramatic change in surface chemistry after ppAm coating with introduction of a broad peak at +1.5 eV characteristic of C-O/C-N/C=N environments as previously reported in ppAm-treated surfaces (22, 35, 37). A peak at +3.0 eV was required to adequately fit the C1s spectrum indicating amides were also present (20, 22, 35, 37). The presence of oxygen environments (CNO/C-O/COOR) could be due to photoelectrons escaping from the PLGA substrate through the ppAm layer. However, oxygen may also be incorporated during plasma polymerization as a result of residual oxygen or H_2O within the reactor or persistent reactive species within the coating reacting with oxygen when exposed to the atmosphere (22, 35, 37).

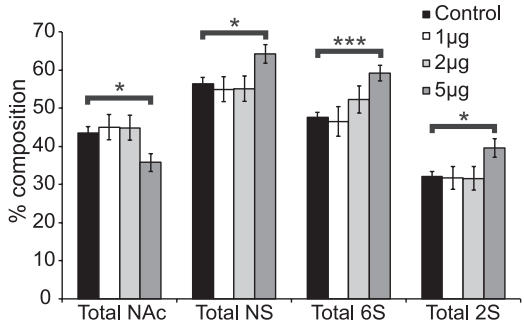

FIGURE 3. **Total sulfation analysis of HS chains bound to ppAm microfiber meshes after incubation with increasing concentrations of HS.** The composition of HS bound to ppAm microfiber scaffolds was determined by soaking 1-cm^2 sections of scaffold with 1, 2, and 5 μg of HS. Bound HS was subsequently removed with 4 M NaCl, and the disaccharide composition was analyzed using RP-HPLC (supplemental Fig. 2*B*) as described previously (24, 25). From the disaccharide analysis, the total levels of *N*-acetylation (*NAc*), *N*-sulfation (*NS*), 6-*O*-sulfation (*6S*), and 2-*O*-sulfation (*2S*) of the bound HS chains could be calculated and are represented in the above chart. Values were statistically compared with the composition of the original HS preparation (control sample) revealing significant increases in total *N*-sulfation (p = 0.022), 6-*O*-sulfation (p = 0.000), and 2-*O*-sulfation (p = 0.021) of HS chains bound to ppAm scaffolds at 5 μg/cm^2. A concomitant significant decrease in *N*-acetylation (p = 0.022) was also observed at this concentration. Values are an average of replicate experiments (control (n = 9); 1 μg (n = 5); 2 μg (n = 4); 5 μg (n = 7)) with *error bars* representing S.E. *, $p < 0.05$; ***, $p < 0.001$.

ppAm-coated plates (20, 21). Uncoated scaffolds showed little if any binding of this probe (Fig. 4*A*); ppAm-coated plates showed dose-dependent binding of the probe with increasing levels of bound heparin (Fig. 4*A*, *inset*). The ppAm-coated scaffolds demonstrated a similar binding profile for GAG-BP to the ppAm-coated plates, indicating that they were similarly able to display heparin in a configuration suitable for protein binding.

We have demonstrated previously that subtle differences in sulfate patterning within HS are important for influencing PSC behavior during differentiation and have suggested that combinations of carefully selected saccharides with specific structural features could be used to direct cell behavior (9, 11). Therefore, it is essential that the three-dimensional conformations of saccharides are retained when they are immobilized onto the spun scaffolds. To assess this, we utilized ScFv antibodies previously used to analyze the presence and distribution of specific sulfation epitopes on the cell surface (9, 33). Two heparin-binding ScFv antibodies, HS4C3 (38, 39) and NS4F5 (40), were able to bind heparin immobilized on ppAm scaffolds (supplemental Fig. 3), demonstrating this GAG was bound in an accessible form and that the method was applicable to the three-dimensional system. Using flow cytometry, we identified that the HS on wild type (E14) mES cells and mES cells deficient in two enzymes involved in HS processing (*Sulf1*$^{-/-}$/*Sulf2*$^{-/-}$), bound the antibody RB4EA12 differentially with significantly greater binding observed in *Sulf1*$^{-/-}$/*2*$^{-/-}$-deficient mES cells (see Fig. 4*B*); this is in good agreement with the known specificity of the antibody for sequences containing 6-sulfation and with the increased content of 6-sulfation in the mutant HS (33).[4] HS chains were isolated from these cell lines and immobilized onto ppAm-coated scaffolds, where analysis with RB4EA12 demonstrated that the difference in binding observed for HS chains when they were attached to proteoglycans on the cell surface was retained when the GAGs were immobilized on the three-dimensional scaffold (Fig. 4*C*).

Binding of GAG-BP to heparin immobilized on ppAm microfiber meshes clearly demonstrates the retention of protein binding capability and confirms the successful functional translation of the ppAm coating to a three-dimensional scaffold. The accessibility of immobilized HS is further reinforced by the differential binding of ScFv antibodies, which verified the retention and presentation of functionally active sulfated motifs within the immobilized HS.

HS Is Retained on the Scaffolds for at Least 10 Days in Culture Conditions—For many applications, cells will need to be grown in contact with GAG-displaying surfaces for extended time periods. We therefore tested the longevity of HS binding to the

[4] R. Holley, unpublished data.

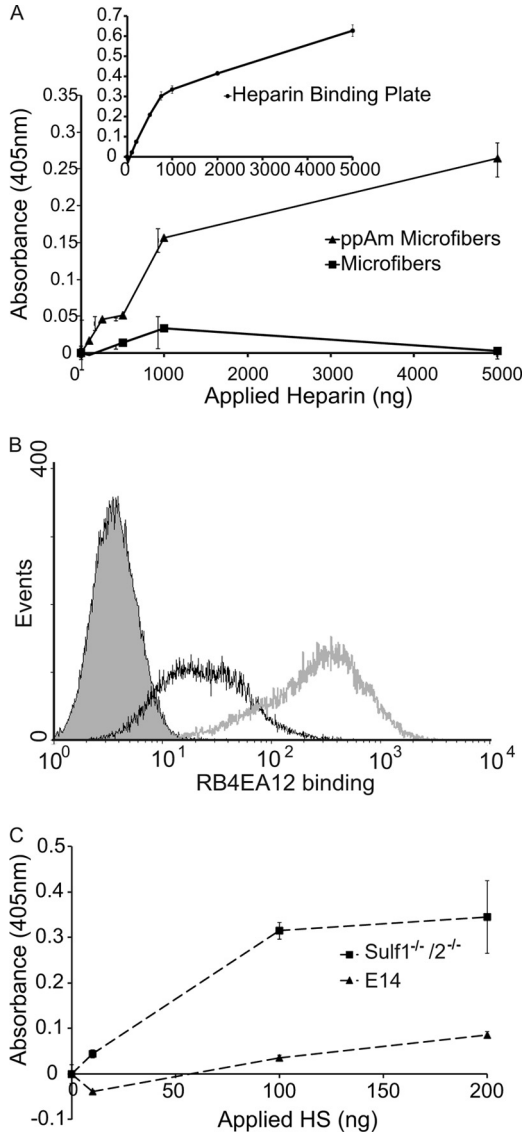

FIGURE 4. **Ligand-binding capability of surface-bound heparin/HS and the use of ScFv antibodies to confirm the presentation of specific sulfation epitopes.** *A*, GAG-BP was used to determine whether surface-bound heparin (immobilized at a range of concentrations) retained its ability to interact with proteins (*i.e.* it was functionally active). *B*, flow cytometry analysis of ScFv antibody RB4EA12 binding to *Sulf1*$^{-/-}$/*2*$^{-/-}$ mES cells (*gray line*) and wild type E14 mES cells (*black line*); *gray-filled peak* represents control data when RB4EA12 was omitted from wild type E14 mES cells. Increased binding of RB4EA12 to *Sulf1*$^{-/-}$/*2*$^{-/-}$ mES cells was observed, indicating RB4EA12 was appropriate for probing the presentation of HS on the surface of ppAm microfiber meshes. *C*, HS derived from E14 wild type mES cells and *Sulf1*$^{-/-}$/*2*$^{-/-}$ mES cells was immobilized on the surface of ppAm scaffolds, and RB4EA12 binding was assessed in a colorimetric assay. RB4EA12 demonstrated increased binding to *Sulf1*$^{-/-}$/*2*$^{-/-}$ HS in agreement with the differential binding observed at the cell surface. Values are the average absorbance for three (*A*) and two (*C*) replicates ± S.E.

scaffold when incubated in PBS over a 10-day period. Although the amount of [^{3}H]HS decreased, 51% of the bound HS remained on the scaffold surface at day 10 (supplemental Fig. 4).

Immobilized HS Can Recover Activity in a HS-deficient Embryonic Stem Cell Line—We have previously demonstrated that *Ext1*$^{-/-}$ deficient (HS-deficient) mES cells cannot commit to neural differentiation unless the medium is continually supplemented with heparin at 1 μg/ml (7). To evaluate the utility of the ppAm scaffolds for display of GAGs in a biologically functional form, scaffolds with immobilized HS were tested for their ability to rescue the neural differentiation capacity of *Ext1*$^{-/-}$ mES cells. Uncoated and ppAm scaffolds were incubated overnight in either PBS with or without HS (1 μg/cm^2). Unbound HS was removed, and scaffolds were washed twice with PBS before overnight conditioning in standard mES medium. Cells were seeded onto the scaffolds in the standard medium (day −1) and after 24 h, medium was replaced with neural induction medium N2B27 (day 0) (31). At day 8, cells on ppAm scaffolds (± HS) had formed large spherical aggregates on the scaffold surface (Fig. 5); cells present on the uncoated scaffold had small granular nuclei, indicative of cell death, revealing that the ppAm coating, even in the absence of bound HS, has improved biocompatibility as reported in previous studies (35, 41). Importantly, ppAm scaffolds with immobilized HS stained positive for the neuronal marker βIII-tubulin, which was present within the aggregates and also in processes that extended out from cell clusters, often interacting with adjacent aggregates. Neural extensions out from the large aggregates were also clearly observed using SEM analysis (supplemental Fig. 5). Conversely, no βIII-tubulin staining was present on ppAm scaffolds without HS. The restoration of *Ext1*$^{-/-}$ neural differentiation confirms the biological activity of bound HS, an outcome that has previously only been achieved by continual addition of soluble HS/heparin to cultures (7, 9).

Neural differentiation of mES cells in N2B27 medium is promoted by autocrine and/or paracrine signaling by FGF4 (31, 42). To investigate whether immobilized HS could enhance neural differentiation by increasing the FGF4 sensitivity of the system, 2 ng/ml FGF4 was added to N2B27 from day 0 (*i.e.* in the above assay) creating four different conditions: +HS/+FGF4 (*i.e.* ppAm-coated scaffold with immobilized HS and soluble FGF4), +HS/−FGF4, −HS/+FGF4, and −HS/−FGF4. After 6 days of culture in N2B27, βIII-tubulin was present in small irregular structures within the cell aggregates cultured in −HS/+FGF4 and +HS/−FGF4, whereas no βIII-tubulin was present in −HS-FGF4 cultures (Fig. 6). In contrast, cells cultured in the presence of both FGF4 and immobilized HS (+HS/+FGF4) had more abundant and extensive βIII-tubulin positive cell projections, *i.e.* with neural processes beginning to extend out from the aggregates over the scaffold surface. This is further supported by quantitative analysis of βIII-tubulin staining in supplemental Fig. 6. At day 8, a low level of βIII-tubulin staining was observed in −HS/−FGF4 culture conditions. This can be attributed to GAGs present in standard mES cell medium in which the cells were seeded and is discussed in more detail in supplemental Fig. 7. However, βIII-tubulin staining of +HS/+FGF4 samples revealed extensive neural differentiation across the entire scaffold surface; with more abundant and mature extensions than in +HS/−FGF4 conditions, extending away from the cell aggregates forming a spread network. This enhanced neural differentiation (and the formation of interconnected neural processes) observed after inclusion of FGF4 suggests that growth factor activity is directly activated by the immobilized HS in this system.

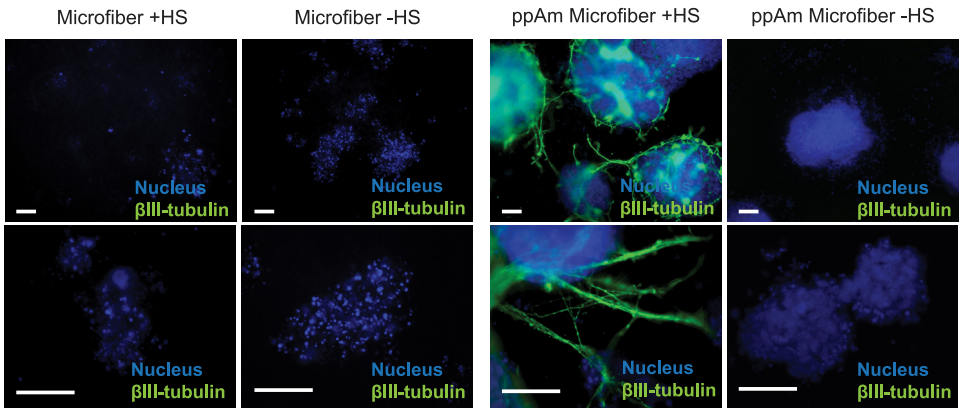

FIGURE 5. **Ext1$^{-/-}$ mES cell neural differentiation on uncoated and ppAm-coated microfiber meshes with or without immobilized HS.** To confirm the biological activity of immobilized HS, *Ext1*$^{-/-}$ mES cells deficient in endogenous HS were seeded onto the surface of ppAm and uncoated microfiber meshes following prior incubation in PBS with (+HS) and without (−HS) HS. Cells were stimulated to differentiate by transfer of scaffolds into N2B27 and stained for βIII-tubulin after 8 days of culture. Positive βIII-tubulin staining was only observed on ppAm microfiber meshes with immobilized HS; βIII-tubulin was present both within the aggregates and in neural processes, which extended out across the scaffold surface. The above images are representative of three separate experiments. *Scale bars*, 50 μm.

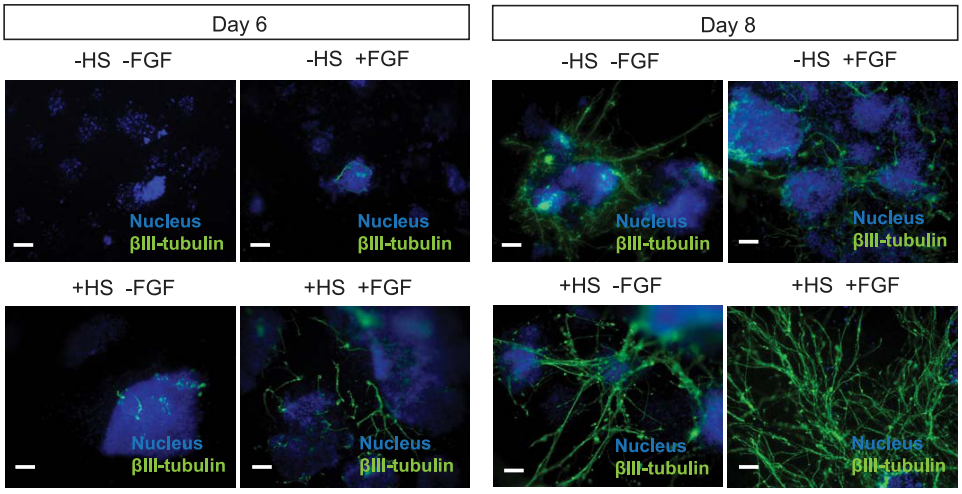

FIGURE 6. **Ext1$^{-/-}$ mES cell neural differentiation on ppAm microfiber meshes with (+HS) and without (−HS) immobilized HS and in the presence (+FGF4) and absence (−FGF4) of FGF4.** Cells were seeded on ppAm microfiber scaffolds with and without HS immobilized and stimulated down a neural lineage with N2B27 medium. FGF4 was added to the differentiation medium from day 0 onwards. Samples were fixed and stained for βIII-tubulin at days 6 and 8. The above images are representative of two separate experiments. The addition of FGF4 appeared to work in synchrony with the immobilized HS to encourage more extensive neural differentiation across the scaffold surface at both time points. Neural differentiation was induced to a very low degree in scaffolds without immobilized HS and FGF4, with the majority of positive staining residing within the cell aggregates. This limited neural differentiation, which was restricted to a few aggregates with irregular, branching structures, is likely to be due to compensation by GAGs present within the standard mES medium in which the scaffolds were preconditioned and the cells were seeded, as discussed in supplemental Fig. 7. Attempts were made to precondition and seed the cells in GAG-free N2B27 medium. However, under these conditions, the cells did not survive the differentiation procedure (not shown). *Ext1*$^{-/-}$mES cells cultured in −HS/+FGF4 developed irregular structures with limited processes across the scaffold surface that can be attributed to the exogenous FGF4 alone combined with residual heparin/HS present within the medium used for initial cell attachment. *Scale bars*, 50 μm.

Immobilized HS Has a Positive Influence on Neural Differentiation of Wild Type mES Cells—To assess the role of HS functionalized meshes in the neural differentiation of wild type ES cells, Wt1 mES cells were seeded on ppAm scaffolds with or without HS and stimulated toward a neural lineage. After 14 days, cells were positive for βIII-tubulin on both surfaces (Fig. 7). However, electrospun meshes with bound HS promote more extensive neural differentiation, most notably in increased neural extensions across the scaffold surface. In comparison, the majority of βIII-tubulin staining appears to be restricted/retained in the large cell aggregates on scaffolds without HS.

Electrospun PLGA meshes have been successfully transformed into functionalized, biocompatible scaffolds that have the capacity to guide PSC behavior. Fundamental functional elements have been sequentially confirmed, including ligand binding capabilities and, most importantly, the presentation of essential sulfated residues implicated in governing PSC differentiation. The combination of ppAm/HS immobilization with electrospun meshes not only restored neural differentiation of *Ext1*$^{-/-}$ mES cells but also appears to enhance the formation of more mature and more highly developed neural processes compared with standard two-dimensional surfaces (supplemental Fig. 8). This combined effect of immobilized HS and scaffold architecture also appears to be translated to wild type mES cells, as evidenced by more abundant neural extensions on ppAm +HS surfaces (Fig. 7). The ability to manipulate microfiber architecture in conjunction with a potential array of immobi-

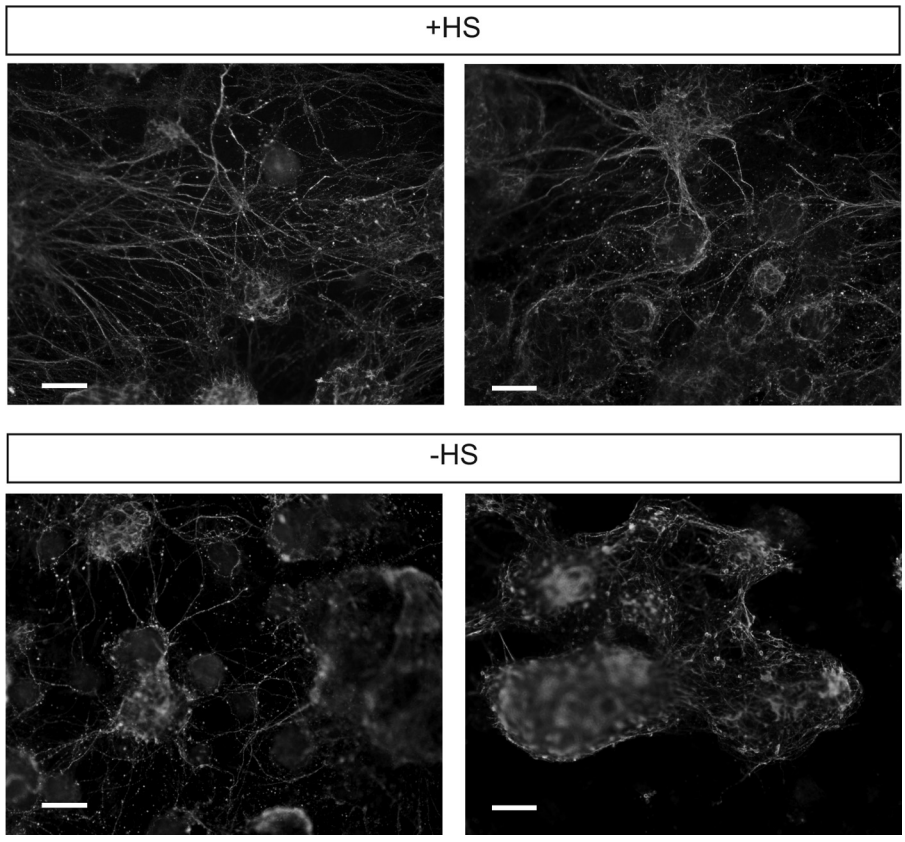

FIGURE 7. **Wt1 mES cell neural differentiation on ppAm microfiber meshes with (+HS) and without (−HS) immobilized HS.** Cells were seeded on ppAm microfiber scaffolds (with and without immobilized HS) and stimulated down a neural lineage with N2B27 medium for 14 days. The above images are representative of two separate experiments. Positive staining for βIII tubulin was observed in both conditions. However, more extensive and elongated neural processes were observed on surfaces with bound HS. In comparison, although a degree of neural extension was observed across the scaffold surface without HS, the majority of staining appears to be localized to the cell aggregates. *Scale bars*, 50 μm.

lized GAGs able to support multiple signaling pathways (43) creates a versatile, bioactive scaffold with far reaching applications for bioengineering and PSC manipulation.

DISCUSSION

This study clearly demonstrates, for the first time, that three-dimensional ECM-mimicking scaffolds (coated by cold plasma polymerization with allylamine) can be easily and rapidly functionalized with the GAG HS with the retention of its biological activity. ppAm-coated surfaces have been used previously to immobilize an array of GAGs (21, 44). Here, we have found that optimized concentrations, where HS immobilization was not influenced by the sulfation motifs present on the heparin/HS chain, were sufficient to illicit a biological response. We therefore fully anticipate the ppAm scaffolds can be utilized to immobilize an equally diverse range of GAG species. This prediction is reinforced by the ability of the ppAm scaffolds to display HS from phenotypically distinct mES cells, preserving and presenting sulfation epitopes that are critical for regulating PSC fate (7, 8, 11).

ppAm coatings have been used previously to ionically immobilize heparin onto stainless steel, improving surface biocompatibility both *in vivo* and *in vitro* and reducing thrombotic activity (41). In contrast, the present study applied ppAm to a three-dimensional, fibrous scaffold for the culture of stem cells. The successful combination of a fibrous ECM-mimicking substrate with biologically active GAGs presented here are highly and broadly applicable to the culture and directed differentiation of PSCs. Our previous research has characterized the role of HS in modulating mES cell behavior, demonstrating that differentiation is accompanied by the generation of specific HS sulfation motifs on cell surface HS proteoglycans (7, 8). This subtle and underexploited control of HS patterning by differentiating cells is the basis for the rigorous examination of bound HS conformation presented in this study, a characterization that has not been previously applied to covalently or non-covalently bound HS in other biological systems (12, 41). By immobilizing selected HS oligosaccharides of a desired length and with distinct sulfation patterning, the scaffolds could be tailored to support the efficient differentiation of PSC cells toward specific cell types (7–9, 11) or promote the differential binding of certain growth factors (45). This is made all the more feasible by recent developments in the chemo-enzymatic synthesis of oligosaccharides of known size, sulfation, and binding activity (46). Supplementation of media with GAGs in standard two-dimensional culture systems involves repeated media changes, which, in turn increases the amount of total GAG used. Although the optimal concentration necessary to mediate a biological response has yet to be determined, the use of immobilized HS has the potential to reduce the total amount of GAG necessary, as demonstrated by enhanced neural process exten-

sion in wild type mES cells cultured on HS functionalized scaffolds. This is particularly important when using synthetic or highly purified GAG preparations and may prove relevant for the differentiation of wild type mES cells (9, 11).

The enhanced neural differentiation observed with FGF4 addition suggests that immobilized HS facilitates growth factor signaling. Considering the broad spectrum of HS binding partners, including numerous growth factors and cytokines, ppAm scaffolds can be easily applied to diverse cell culture environments. In addition, the ability of the immobilized HS to mediate the activity of FGF4 at minimal concentrations (2 ng/ml) (31) indicates that the scaffold format developed here will be particularly relevant in the creation of defined PSC culture systems, particularly human ES cell culture where supplementation with FGF2 can range between 4–100 ng/ml (47).

The benefits of utilizing immobilized HS to manipulate PSC behavior is further reinforced by the increased extension of neural processes across the scaffold surface in wild type mES cells on surfaces with bound HS. The behavior of PSCs is dependent on a complex interplay of numerous factors, including mechanical cues, scaffold architecture, and growth factor signaling. Therefore, the exact mechanisms behind this enhancement need to be explored further to yield optimum effects.

Our scaffolds possess the unique combination of microfibers functionalized with non-covalently bound, biologically active GAGs. The use of an electrospun mesh offers another level of flexibility in terms of manipulating the PSC pericellular environment. Their fibrous structure can assist the maintenance of PSC pluripotency (14, 16) and enhance differentiation (12). Consistent with these reports, our results revealed more developed neural differentiation on the microfiber meshes compared with standard tissue culture plastic (*i.e.* a two-dimensional format). Fiber size and orientation can also be easily manipulated (12) such that when aligned fibers are coated with immobilized HS, this may lead to orientated and enhanced elongation of neural processes. Therefore, the combination of ppAm electrospun meshes with immobilized GAGs have the potential to generate a powerful and dynamic biomaterial, which will prove valuable in elucidating the requirements for defined, reproducible, scalable and cost effective human ES/induced pluripotent stem cell culture systems.

As highly porous, flexible ECM mimics, electrospun meshes have received considerable attention as vehicles for therapeutic cell delivery or as an instructive matrix to facilitate healing of endogenous tissue. In this regard, ppAm meshes functionalized with specialized GAG preparations have extensive therapeutic potential, including wound healing (48), vascular tissue engineering (49), and neural repair (12). Alternative approaches to GAG incorporation include spinning into fibers and covalent immobilization on the fiber surface (49). Incorporation into the mesh causes a release of heparin/HS into the immediate microenvironment, which is desirable for certain applications (49), whereas covalent modification can have varying degrees of efficiency and may alter the functional properties of particular GAG preparations (12). In the current study, we aimed to mimic the presentation of HS by native HS proteoglycans, where HS chains project out from a central core protein. This approach is beneficial compared with GAG applied in solution as the HS/heparin is localized to the cell microenvironment, which may in turn enhance biological activity as has been reported for tethered growth factors (12, 16, 50). Immobilization of GAGs via plasma polymerized treated surfaces can be applied to a variety of therapeutically relevant materials and scaffold structures (35, 41) and also raises the possibility of introducing functional gradients of ppAm and therefore HS/heparin (28) that may be used to manipulate cell behavior both *in vivo* and *in vitro*. Fundamentally, it is a readily scalable process, which is an essential quality if scaffolds are to be applied to PSC culture or developed as therapeutic devices.

Here, we have successfully coated heparin/HS onto a three-dimensional scaffold without chemical modification and in an orientation that ensured motifs implicated in biological function and ligand binding were accessible. This approach creates a highly flexible, tunable scaffold, which can be adapted for the culture of diverse cell types, providing many of the characteristics of the native ECM but allowing the controlled application of specific, active GAG saccharides to influence cell behavior.

Acknowledgment—We thank Douglas Dyer for production of GAG-BP.

REFERENCES

1. Ludwig, T. E., Levenstein, M. E., Jones, J. M., Berggren, W. T., Mitchen, E. R., Frane, J. L., Crandall, L. J., Daigh, C. A., Conard, K. R., Piekarczyk, M. S., Llanas, R. A., and Thomson, J. A. (2006) Derivation of human embryonic stem cells in defined conditions. *Nat. Biotechnol.* **24,** 185–187
2. Baxter, M. A., Camarasa, M. V., Bates, N., Small, F., Murray, P., Edgar, D., and Kimber, S. J. (2009) Analysis of the distinct functions of growth factors and tissue culture substrates necessary for the long-term self-renewal of human embryonic stem cell lines. *Stem Cell Res.* **3,** 28–38
3. Bateman, K. L., Delehedde, M., Sergeant, N., Wartelle, I., Vidyasagar, R., and Fernig, D. G. (2000) Heparan sulphate. Regulation of growth factors in the mammary gland. *Adv. Exp. Med. Biol.* **480,** 65–69
4. Macri, L., Silverstein, D., and Clark, R. A. (2007) Growth factor binding to the pericellular matrix and its importance in tissue engineering. *Adv. Drug Deliv. Rev.* **59,** 1366–1381
5. Harmer, N. J. (2006) Insights into the role of heparan suphate in fibroblast growth factor signalling. *Biochem. Soc. Trans.* **34,** 442–445
6. Esko, J. D., and Lindahl, U. (2001) Molecular diversity of heparan sulfate. *J. Clin. Invest.* **108,** 169–173
7. Johnson, C. E., Crawford, B. E., Stavridis, M., Ten Dam, G., Wat, A. L., Rushton, G., Ward, C. M., Wilson, V., van Kuppevelt, T. H., Esko, J. D., Smith, A., Gallagher, J. T., and Merry, C. L. (2007) Essential alterations of heparan sulfate during the differentiation of embryonic stem cells to Sox1-enhanced green fluorescent protein-expressing neural progenitor cells. *Stem Cells* **25,** 1913–1923
8. Baldwin, R. J., ten Dam, G. B., van Kuppevelt, T. H., Lacaud, G., Gallagher, J. T., Kouskoff, V., and Merry, C. L. (2008) A developmentally regulated heparan sulfate epitope defines a subpopulation with increased blood potential during mesodermal differentiation. *Stem Cells* **26,** 3108–3118
9. Pickford, C. E., Holley, R. J., Rushton, G., Stavridis, M. P., Ward, C. M., and Merry, C. L. (2011) Specific glycosaminoglycans modulate neural specification of mouse embryonic stem cells. *Stem Cells* **29,** 629–640
10. Helledie, T., Dombrowski, C., Rai, B., Lim, Z. X., Hin, I. L., Rider, D. A., Stein, G. S., Hong, W., van Wijnen, A. J., Hui, J. H., Nurcombe, V., and Cool, S. M. (2012) Heparan sulfate enhances the self-renewal and therapeutic potential of mesenchymal stem cells from human adult bone marrow. *Stem Cells Dev.* **21,** 1897–1910
11. Holley, R. J., Pickford, C. E., Rushton, G., Lacaud, G., Gallagher, J. T., Kouskoff, V., and Merry, C. L. (2011) Influencing hematopoietic differen-

tiation of mouse embryonic stem cells using soluble heparin and heparan sulfate saccharides. *J. Biol. Chem.* **286,** 6241–6252
12. Lam, H. J., Patel, S., Wang, A., Chu, J., and Li, S. (2010) In vitro regulation of neural differentiation and axon growth by growth factors and bioactive nanofibers. *Tissue Eng. Part A* **16,** 2641–2648
13. Engler, A. J., Sen, S., Sweeney, H. L., and Discher, D. E. (2006) Matrix elasticity directs stem cell lineage specification. *Cell* **126,** 677–689
14. Nur-E-Kamal, A., Ahmed, I., Kamal, J., Schindler, M., and Meiners, S. (2006) Three-dimensional nanofibrillar surfaces promote self-renewal in mouse embryonic stem cells. *Stem Cells* **24,** 426–433
15. Kim, T. G., and Park, T. G. (2006) Biomimicking extracellular matrix: cell adhesive RGD peptide modified electrospun poly(D,L-lactic-co-glycolic acid) nanofiber mesh. *Tissue Eng.* **12,** 221–233
16. Nur-E-Kamal, A., Ahmed, I., Kamal, J., Babu, A. N., Schindler, M., and Meiners, S. (2008) Covalently attached FGF-2 to three-dimensional polyamide nanofibrillar surfaces demonstrates enhanced biological stability and activity. *Mol. Cell Biochem.* **309,** 157–166
17. Sørensen, V., Nilsen, T., and Wiedłocha, A. (2006) Functional diversity of FGF-2 isoforms by intracellular sorting. *Bioessays* **28,** 504–514
18. Pike, D. B., Cai, S., Pomraning, K. R., Firpo, M. A., Fisher, R. J., Shu, X. Z., Prestwich, G. D., and Peattie, R. A. (2006) Heparin-regulated release of growth factors *in vitro* and angiogenic response *in vivo* to implanted hyaluronan hydrogels containing VEGF and bFGF. *Biomaterials* **27,** 5242–5251
19. Park, K., Cho, K. J., Kim, J. J., Kim, I. H., and Han, D. K. (2009) Functional PLGA scaffolds for chondrogenesis of bone-marrow-derived mesenchymal stem cells. *Macromol. Biosci.* **9,** 221–229
20. Mahoney, D. J., Whittle, J. D., Milner, C. M., Clark, S. J., Mulloy, B., Buttle, D. J., Jones, G. C., Day, A. J., and Short, R. D. (2004) A method for the non-covalent immobilization of heparin to surfaces. *Anal. Biochem.* **330,** 123–129
21. Marson, A., Robinson, D. E., Brookes, P. N., Mulloy, B., Wiles, M., Clark, S. J., Fielder, H. L., Collinson, L. J., Cain, S. A., Kielty, C. M., McArthur, S., Buttle, D. J., Short, R. D., Whittle, J. D., and Day, A. J. (2009) Development of a microtiter plate-based glycosaminoglycan array for the investigation of glycosaminoglycan-protein interactions. *Glycobiology* **19,** 1537–1546
22. Robinson, D. E., Buttle, D. J., Short, R. D., McArthur, S. L., Steele, D. A., and Whittle, J. D. (2012) Glycosaminoglycan (GAG) binding surfaces for characterizing GAG-protein interactions. *Biomaterials* **33,** 1007–1016
23. Aviss, K. J., Gough, J. E., and Downes, S. (2010) Aligned electrospun polymer fibres for skeletal muscle regeneration. *Eur. Cell Mater.* **19,** 193–204
24. Deakin, J. A., and Lyon, M. (2008) A simplified and sensitive fluorescent method for disaccharide analysis of both heparan sulfate and chondroitin/dermatan sulfates from biological samples. *Glycobiology* **18,** 483–491
25. Holley, R. J., Deligny, A., Wei, W., Watson, H. A., Niñonuevo, M. R., Dagälv, A., Leary, J. A., Bigger, B. W., Kjellén, L., and Merry, C. L. (2011) Mucopolysaccharidosis type I, unique structure of accumulated heparan sulfate and increased *N*-sulfotransferase activity in mice lacking α-l-iduronidase. *J. Biol. Chem.* **286,** 37515–37524
26. Parkar, A. A., Kahmann, J. D., Howat, S. L., Bayliss, M. T., and Day, A. J. (1998) TSG-6 interacts with hyaluronan and aggrecan in a pH-dependent manner via a common functional element: implications for its regulation in inflamed cartilage. *FEBS Lett.* **428,** 171–176
27. Mahoney, D. J., Mulloy, B., Forster, M. J., Blundell, C. D., Fries, E., Milner, C. M., and Day, A. J. (2005) Characterization of the interaction between tumor necrosis factor-stimulated gene-6 and heparin: implications for the inhibition of plasmin in extracellular matrix microenvironments. *J. Biol. Chem.* **280,** 27044–27055
28. Robinson, D. E., Marson, A., Short, R. D., Buttle, D. J., Day, A. J., Parry, K. L., Wiles, M., Highfield, P., Mistry, A., and Whittle, J. D. (2008) Surface gradient of functional heparin. *Advanced Materials* **20,** 1166–1169
29. van Kuppevelt, T. H., Dennissen, M. A., van Venrooij, W. J., Hoet, R. M., and Veerkamp, J. H. (1998) Generation and application of type-specific anti-heparan sulfate antibodies using phage display technology. Further evidence for heparan sulfate heterogeneity in the kidney. *J. Biol. Chem.* **273,** 12960–12966
30. Lin, X., Wei, G., Shi, Z., Dryer, L., Esko, J. D., Wells, D. E., and Matzuk, M. M. (2000) Disruption of gastrulation and heparan sulfate biosynthesis in EXT1-deficient mice. *Dev. Biol.* **224,** 299–311
31. Ying, Q. L., Stavridis, M., Griffiths, D., Li, M., and Smith, A. (2003) Conversion of embryonic stem cells into neuroectodermal precursors in adherent monoculture. *Nat. Biotechnol.* **21,** 183–186
32. Merry, C. L., Bullock, S. L., Swan, D. C., Backen, A. C., Lyon, M., Beddington, R. S., Wilson, V. A., and Gallagher, J. T. (2001) The molecular phenotype of heparan sulfate in the Hs2st-/- mutant mouse. *J. Biol. Chem.* **276,** 35429–35434
33. Lamanna, W. C., Baldwin, R. J., Padva, M., Kalus, I., Ten Dam, G., van Kuppevelt, T. H., Gallagher, J. T., von Figura, K., Dierks, T., and Merry, C. L. (2006) Heparan sulfate 6-*O*-endosulfatases: discrete *in vivo* activities and functional cooperativity. *Biochem. J.* **400,** 63–73
34. Stevens, M. M., and George, J. H. (2005) Exploring and engineering the cell surface interface. *Science* **310,** 1135–1138
35. Barry, J. J., Silva, M. M., Shakesheff, K. M., Howdle, A. M., and Alexander, M. (2005) Plasma deposits to promote cell population of the porous interior of three-dimensional poly(D,L-lactic acid) tissue-engineering scaffolds. *Advanced Functional Materials* **15,** 1134–1140
36. Beamson, G., and Briggs, D. (1992) *High Resolution XPS of Organic Polymers*, Wiley, New York
37. Shard, A. G., Whittle, J. D., Beck, A. J., Brookes, P. N., Bullett, N. A., Talib, R. A., Mistry, A., Barton, D., and McArthur, S. L. (2004) A NEXAFS examination of unsaturation in plasma polymers of allylamine and propylamine. *J. Phys. Chem. B* **108,** 12472–12480
38. Smits, N. C., Lensen, J. F., Wijnhoven, T. J., Ten Dam, G. B., Jenniskens, G. J., and van Kuppevelt, T. H. (2006) Phage display-derived human antibodies against specific glycosaminoglycan epitopes. *Methods Enzymol.* **416,** 61–87
39. Ten Dam, G. B., Kurup, S., van de Westerlo, E. M., Versteeg, E. M., Lindahl, U., Spillmann, D., and van Kuppevelt, T. H. (2006) 3-*O*-sulfated oligosaccharide structures are recognized by anti-heparan sulfate antibody HS4C3. *J. Biol. Chem.* **281,** 4654–4662
40. Wijnhoven, T. J., van de Westerlo, E. M., Smits, N. C., Lensen, J. F., Rops, A. L., van der Vlag, J., Berden, J. H., van den Heuvel, L. P., and van Kuppevelt, T. H. (2008) Characterization of anticoagulant heparinoids by immunoprofiling. *Glycoconj. J.* **25,** 177–185
41. Yang, Z., Tu, Q., Wang, J., and Huang, N. (2012) The role of heparin binding surfaces in the direction of endothelial and smooth muscle cell fate and re-endothelialization. *Biomaterials* **33,** 6615–6625
42. Stavridis, M. P., Lunn, J. S., Collins, B. J., and Storey, K. G. (2007) A discrete period of FGF-induced Erk1/2 signalling is required for vertebrate neural specification. *Development* **134,** 2889–2894
43. Smith, R. A., Meade, K., Pickford, C. E., Holley, R. J., and Merry, C. L. (2011) Glycosaminoglycans as regulators of stem cell differentiation. *Biochem. Soc. Trans.* **39,** 383–387
44. Clark, S. J., Higman, V. A., Mulloy, B., Perkins, S. J., Lea, S. M., Sim, R. B., and Day, A. J. (2006) His-384 allotypic variant of factor H associated with age-related macular degeneration has different heparin binding properties from the non-disease-associated form. *J. Biol. Chem.* **281,** 24713–24720
45. Gallagher, J. T. (2001) Heparan sulfate: growth control with a restricted sequence menu. *J. Clin. Invest.* **108,** 357–361
46. Xu, Y., Masuko, S., Takieddin, M., Xu, H., Liu, R., Jing, J., Mousa, S. A., Linhardt, R. J., and Liu, J. (2011) Chemoenzymatic synthesis of homogeneous ultralow molecular weight heparins. *Science* **334,** 498–501
47. Xu, R. H., Peck, R. M., Li, D. S., Feng, X., Ludwig, T., and Thomson, J. A. (2005) Basic FGF and suppression of BMP signaling sustain undifferentiated proliferation of human ES cells. *Nat. Methods* **2,** 185–190
48. Kurpinski, K. T., Stephenson, J. T., Janairo, R. R., Lee, H., and Li, S. (2010) The effect of fiber alignment and heparin coating on cell infiltration into nanofibrous PLLA scaffolds. *Biomaterials* **31,** 3536–3542
49. Spadaccio, C., Rainer, A., Centola, M., Trombetta, M., Chello, M., Lusini, M., Covino, E., Toyoda, Y., and Genovese, J. A. (2010) Heparin-releasing scaffold for stem cells: a differentiating device for vascular aims. *Regen. Med.* **5,** 645–657
50. Fan, V. H., Tamama, K., Au, A., Littrell, R., Richardson, L. B., Wright, J. W., Wells, A., and Griffith, L. G. (2007) Tethered epidermal growth factor provides a survival advantage to mesenchymal stem cells. *Stem Cells* **25,** 1241–1251